Indian Journal of Chemistry
Vol. 62, April 2023, pp. 401-410
DOI: 10.56042/ijc.v62i4.447

Density functional analysis of molecular crystal: bis-l-Phenyl alanine mandelate

S Usha[a,*] & Charles Kanakam Christopher[b]

[a] Department of Chemistry, Sri Sairam Engineering College, Chennai 600 044, India
[b] Department of Chemistry, Presidency College, Chennai 600 005, India

*E-mail: usha.che@sairam.edu.in

Received 28 September 2021; accepted (revised) 10 March 2023

A novel organic nonlinear four component molecular crystal bis-l-phenylalanine mandelate (BLPAMA) has been synthesized and single crystal has been grown by slow evaporation method in an aqueous solution at ambient temperature. The characterization studies support the formation of the neutral novel organic molecular crystal containing 68 atoms in a molecule. The experimental and theoretical density functional analysis (DFT) have been compared for the vibrational changes, dipolar interactions, ^{1}H and ^{13}C NMR values, UV-visible absorption pattern, HOMO-LUMO interactions, hyperconjugation effects, Natural Bond Orbital (NBO) and Natural Hybridisation Orbital (NHO) analysis. The molecular structure obtained from the solid state experimental data using ORTEP diagram has been compared with the gaseous state optimized stucture obtained from DFT data using Gaussian 98 software with MO6-31++(d,p) basis set. The DFT study of the title compound has confirmed the crystal formation through charge transfer mechanism, hydrogen bonding interactions and van der Waals forces of attraction. The stress and strain in the title compound leads to the low energy gap nonlinear molecular sheet formation. The title compound shows electrochemical activity due to the highly reactive and relatively unstable structure.

Keywords: Molecular crystal, BLPAMA, NBO, NHO, HOMO-LUMO

The alpha hydroxy phenyl acetic acid, mandelic acid (MA) found many applications in curing skin diseases, acne and photo-aging. The essential amino acid l-phenylalanine (LPA) found in dietary intakes is also found in many of the biological application in our routine life. Both MA and LPA have non-centrosymmetric structure. The combination of MA and LPA in different molar ratios resulted in the formation of novel organic complex salts. An organic salt, BLPAMA contains four components namely two molecules of phenyl alanine (PA), one molecule of mandelic acid (MA) and one molecule of water in the crystal. The single crystal XRD study in the solid state showed the presence of $P2_1$ space group is shown in the Fig. 1 ORTEP diagram[1] and it is compared with the theoretical gaseous phase molecular parameters arrived at using Gaussian 98 software with MO6-31++(d,p) basis set and are discussed in detail[2]. Optimized structure of BLPAMA in two different views are shown in Fig. 2 and Fig. 3.

The restricted movement of atoms in the solid state decreases the bond length values compared to the increase in entropy in the gaseous state DFT measurement increases the bond length values which almost coincide with the expected bond lengths of respective bonds as shown in Table 1. Thus the experimental bond lengths are lower compared to the theoretical bond lengths[3]. Heteroatomic charge transfer mechanism increases the bond lengths in the DFT measurements shown in the bonding of N1-H19, N2-H29, O8-H31, C14-H13, O1-H31.

The in plane bending, out of plane bending, twisting occurring in the BLPAMA molecule in the gaseous state in Table 2, show the theoretical bond angles are lesser than the experimental values which indicate the delocalisation of charges in the gaseous phase.

The torsional angles in Table 3, indicate the charge transfer mechanism leading to the strong hydrogen bonding interactions. This results in the low dihedral angle values in both the solid phase and gaseous phase. The clockwise rotation about the dihedral axis and the counter clockwise rotation about the dihedral axis results in positive and negative values for dihedral angle values respectively.

The distance between the donor atoms oxygen and nitrogen and acceptor hydrogen shows lesser experimental value indicating a stronger hydrogen

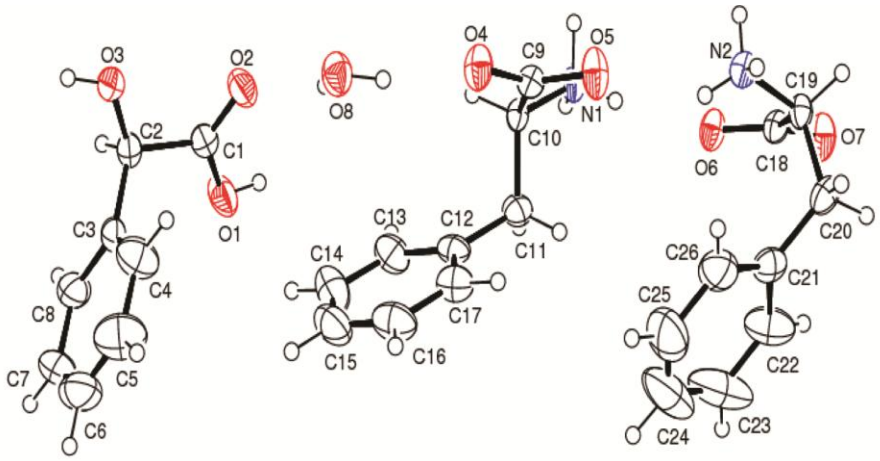

Fig. 1 — Molecular crystal structure of BPLAMA

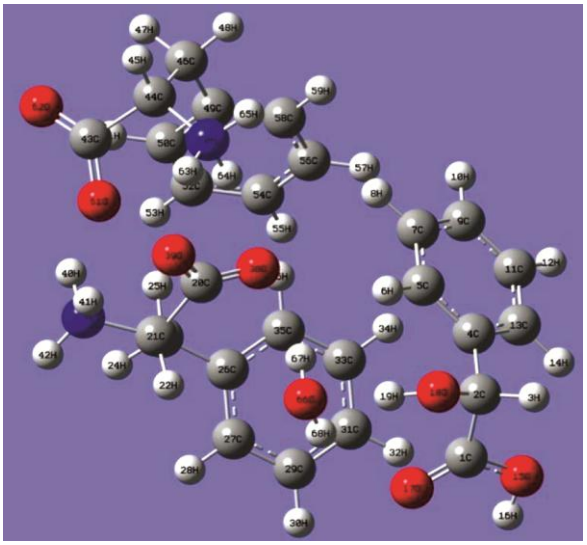

Fig. 2 — BLPAMA DFT optimised structure - view 1

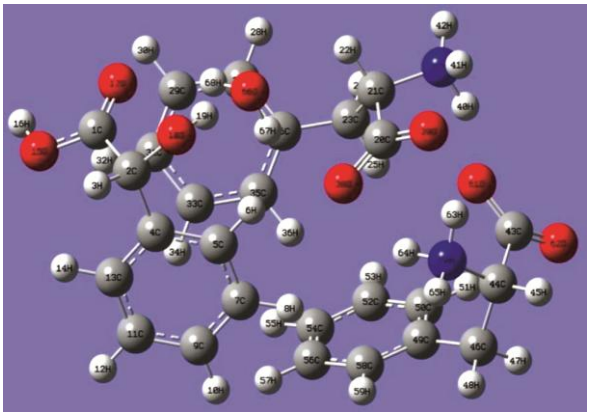

Fig. 3 — BLPAMA DFT optimized structure - view 2

bonding interaction, the expected donor acceptor distance for hydrogen bonds is 2.7-3.3. Theoretical values of distance between the donor hydrogen and acceptoroxygen shows lower values for the N1-H17.....O6, O5-H28.....N2 hydrogen bonds due to the strong hydrogen bonding interactions in the molecule[4]. The lower theoretical donor -hydrogen-acceptor angle values due to measurement of the disorderly gaseous phase for the compound are shown in Table 4.

The 68 atoms present in the BLPAMA crystal show the neutral charged molecule and are confirmed by the Mulliken atomic charge values shown in Table 5. The initial values indicate the single crystal XRD input cif file measurements and the final values are the atomic charge values for the optimised geometrical structure during DFT measurement. The negative charges are indicating the charge transfer during the donor-acceptor interactions. Vibrational changes happening in the organic salt using FTIR solid state measurement is compared with the gaseous phase DFT calculation. The relative deviation obtained from both the methods show negative values for the bond types involved in the charge transfer namely C-N bond, C-O bond and N-H bond. FTIR band assignment, reduced mass, force constant and intensity values with respect to vibrational assignments are shown in Table 6. The FTIR spectrum of BLPAMA is shown in the Fig. 4. The stretching and bending vibrations are comparable and the intensity observed in the FTIR measurements are matching with that of DFT measurements except for the linkages involving charge transfer are shown in the Table 7.

Raman scattering and polarizability

Raman Spectrum Fig. 5 supports the vibrational rotational changes noticed in FT-IR of the title compound, the slight increase in the respective values in the Raman spectra indicates the presence of charge

Table 1 — BLPAMA bond length (Å)

Atoms	Experimental	Theoretical	Atoms	Experimental	Theoretical
C1-C2	1.507	1.525	C15-H14	0.930	1.089
C1-O1	1.298	1.344	C15-C16	1.359	1.391
C1-O2	1.197	1.209	C16-H15	0.929	1.090
C2-H1	0.980	1.101	C16-C17	1.375	1.390
C2-C3	1.505	1.529	C17-H16	0.931	1.088
C2-O3	1.407	1.381	N1-H17	0.895	1.064
C3-C4	1.366	1.392	N1-H18	1.006	1.035
C3-C8	1.359	1.398	N1-H19	0.884	1.017
C4-H2	0.930	1.086	O4-H31	1.809	1.977
C4-C5	1.369	1.391	O5-H28	2.101	1.819
C5-H3	0.930	1.089	H17-O6	1.955	1.617
C5-C6	1.344	1.389	C18-C19	1.514	1.553
C6-H4	0.930	1.089	C18-O6	1.244	1.265
C6-C7	1.330	1.394	C18-O7	1.240	1.226
C7-H5	0.930	1.088	C19-H20	0.980	1.096
C7-C8	1.378	1.389	C19-C20	1.519	1.526
C8-H6	0.930	1.089	C19-N2	1.475	1.497
O1-H7	0.820	0.970	C20-H21	0.970	1.096
O1-H13	2.888	4.715	C20-H22	0.970	1.100
O2-H32	2.400	2.096	C20-C21	1.495	1.508
O3-H8	0.820	0.984	C21-C22	1.371	1.400
C9-C10	1.520	1.548	C21-C26	1.370	1.396
C9-O4	1.227	1.248	C22-H23	0.929	1.089
C9-O5	1.250	1.257	C22-C23	1.361	1.389
C10-H9	0.981	1.099	C23-H24	0.930	1.087
C10-C11	1.520	1.530	C23-C24	1.372	1.393
C10-N1	1.486	1.502	C24-H25	0.930	1.088
C11-H10	0.970	1.102	C24-C25	1.358	1.389
C11-H11	0.971	1.098	C25-H26	0.931	1.088
C11-C12	1.499	1.504	C25-C26	1.360	1.393
C12-C13	1.373	1.396	C26-H27	0.930	1.092
C12-C17	1.376	1.394	N2-H28	0.827	1.049
C13-H12	0.930	1.091	N2-H29	0.906	1.035
C13-C14	1.370	1.390	N2-H30	0.922	1.021
C14-H13	0.930	1.087	O8-H31	0.858	0.974
C14-C15	1.368	1.393	O8-H32	0.854	0.969

Table 2 — BLPAMA bond angle (Å)

Atoms	Experimental	Theoretical	Atoms	Experimental	Theoretical
C1-O1-H7	109.440	106.227	C10-N1-H17	112.675	106.378
C1-O1-H13	89.786	61.033	C10-N1-H18	110.662	103.733
H7-O1-H13	91.947	53.130	C10-N1-H19	109.646	114.788
C1-O2-H32	131.358	116.673	H17-N1-H18	105.982	103.622
C9-C10-N1	109.834	103.546	H17-N1-H19	106.483	113.578
O1-H13-C14	140.364	82.482	H18-N1-H19	111.294	113.621
O2-H32-O8	152.092	135.658	C9-O4-H31	131.266	98.802
C19-N2-H29	108.120	111.654	C9-O5-H28	150.535	93.605
C19-N2-H30	106.956	112.967	N1-H17-O6	156.244	145.306
O8-H31-H32	108.799	105.980	H17-O6-C18	152.692	149.707
O4-O8-H31	166.011	144.811	O5-H28-N2	136.825	148.050

transfer mechanism existing between donor - acceptor atoms[5] resulting in polarizability in the moleculeis given in the Table 8.

NPA analysis in Table 9, shows the presence of four molecular units in the crystal, the composition of Lewis electrons, valence non - Lewis electrons,

Table 3 — BLPAMA dihedral angle (Å)

Atoms	Experimental	Theoretical	Atoms	Experimental	Theoretical
O2-C1-C2-O3	1.844	27.914	H12-C12-C14-C15	178.372	-179.437
C2-C1-O1-H7	165.740	-177.920	C12-C14-H13-O1	-32.300	-137.972
C2-C1-O1-H13	-102.271	-149.009	C15-C14-H13-O1	147.664	40.867
O2-C1-O1-H7	-13.066	1.700	C12-C14-C15-H14	-178.413	178.510
O2-C1-O1-H13	78.924	30.611	H14-C15-C16-C17	179.224	-178.330
C2-C1-O2-H32	93.630	29.436	C15-C16-C17-H16	-179.818	178.290
O1-C1-O2-H32	-87.717	-150.129	C1-C2-O3-H8	160.371	-55.599
C1-C2-C3-C4	69.561	117.836	H1-C2-O3-H8	43.352	-171.424
C1-C2-C3-C8	-111.816	-63.352	C3-C2-O3-H8	-75.650	68.832
H1-C2-C3-C4	-171.125	-127.464	C8-C3-C4-H2	179.071	-179.146
H1-C2-C3-C8	7.497	51.348	C4-C3-C8-H6	-179.143	179.758
O3-C2-C3-C4	-52.141	-7.795	C3-C4-C5-H3	-178.780	178.095
O3-C2-C3-C8	126.482	171.017	H2-C4-C5-C6	-178.786	178.415
C13-C12-C17-C16	-0.185	-1.018	C4-C5-C6-H4	178.614	-178.232
C13-C12-C17-H16	179.687	-179.308	H3-C5-C6-C7	178.618	-178.291
C6-C7-C8-H6	178.944	-179.958	C10-N1-H17-O6	153.773	-41.829
C1-O1-H13-C14	-73.183	61.424	H18-N1-H17-O6	-85.066	67.186
H7-O1-H13-C14	36.262	-154.043	H19-N1-H17-O6	33.534	-169.063
C1-O2-H32-O8	-94.994	-45.867	C9-O4-H31-O8	-143.742	-37.561
O4-C9-C10-N1	148.858	-152.759	C9-O5-H28-N2	147.781	-1.201
O5-C9-O4-H31	-177.544	125.550	N1-H17-O6-C18	134.952	-131.860
C10-C9-O5-H28	-11.642	-126.953	O6-C18-C19-H20	-140.172	-125.846
O4-C9-O5-H28	165.723	48.887	O7-C18-C19-N2	159.567	173.860
C9-C10-N1-H17	59.290	71.842	C19-C18-O6-H17	27.709	133.565
C9-C10-N1-H18	-59.165	-37.095	O7-C18-O6-H17	-154.198	-49.437
C9-C10-N1-H19	177.693	-161.649	C18-C19-C20-H22	-179.379	174.452
H9-C10-N1-H17	178.695	-172.982	H20-C19-C20-C21	-175.700	178.100
H9-C10-N1-H18	178.812	-160.302	C18-C19-N2-H28	48.935	-49.847
C11-C12-C17-C16	-179.174	178.141	C18-C19-N2-H29	171.698	63.515
H24-C23-C24-C25	177.346	-179.824	C18-C19-N2-H30	-70.332	-175.309
C23-C24-C25-H26	-177.788	179.308	H20-C19-N2-H28	166.948	68.119
C24-C25-C26-H27	179.887	-179.016	H20-C19-N2-H29	-70.289	-178.519
C19-N2-H28-O5	-169.650	119.884	H20-C19-N2-H30	47.681	-57.343
H29-N2-H28-O5	69.716	0.143	C20-C19-N2-H28	-74.402	-172.318
H30-N2-H28-O5	-51.923	-112.656	C20-C19-N2-H29	48.361	-58.956
H31-O8-H32-O2	-168.438	111.920	C20-C19-N2-H30	166.331	62.220
H23-C22-C23-C24	-178.867	179.415	C26-C21-C22-H23	-179.009	179.702

Table 4 — BLPAMA hydrogen bonds

D – H….. A	d(D-H)		d(H…..A)		d(D…..A)		∠DHA	
	Expt.	Theo.	Expt.	Theo.	Expt.	Theo.	Expt.	Theo.
N1-H17.....O6	0.895	1.064	1.955	1.617	2.850	2.681	156.244	145.306
O5-H28.....N2	0.827	1.049	2.101	1.819	2.928	2.868	136.825	148.050
O4-O8....H31	0.858	0.974	1.809	1.977	2.667	2.951	166.011	144.811
O2-H32....O8	0.854	0.969	2.400	2.096	3.254	3.065	152.092	135.658

Table 5 — BLPAMA Mulliken atomic charges

Atom	Atom	Initial	Final	Atom No	Atom	Initial	Final
1	C	0.590	0.603	35	C	-0.078	-0.052
2	C	0.020	0.056	36	H	0.066	0.067
3	H	0.133	0.157	37	N	-0.501	-0.609
4	C	0.093	0.061	38	O	-0.535	-0.615

(*Contd.*)

Table 5 — BLPAMA Mulliken atomic charges (*Contd*.)

Atom	Atom	Initial	Final	Atom No	Atom	Initial	Final
5	C	-0.102	-0.119	39	O	-0.641	-0.630
6	H	0.120	0.127	40	H	0.324	0.382
7	C	-0.097	-0.072	41	H	0.357	0.357
8	H	0.099	0.069	42	H	0.329	0.332
9	C	-0.080	-0.116	43	C	0.592	0.634
10	H	0.098	0.097	44	C	-0.175	-0.107
11	C	-0.089	-0.130	45	H	0.174	0.167
12	H	0.095	0.118	46	C	-0.297	-0.302
13	C	-0.133	-0.129	47	H	0.180	0.184
14	H	0.082	0.121	48	H	0.132	0.113
15	O	-0.432	-0.507	49	C	0.095	0.081
16	H	0.298	0.347	50	C	-0.093	-0.121
17	O	-0.462	-0.500	51	H	0.106	0.153
18	O	-0.503	-0.585	52	C	-0.092	-0.130
19	H	0.295	0.361	53	H	0.102	0.129
20	C	0.584	0.682	54	C	-0.097	-0.115
21	C	-0.127	-0.106	55	H	0.099	0.126
22	H	0.152	0.180	56	C	-0.087	-0.092
23	C	-0.260	-0.269	57	H	0.101	0.101
24	H	0.128	0.111	58	C	-0.117	-0.153
25	H	0.141	0.147	59	H	0.061	0.092
26	C	0.106	0.096	60	N	-0.422	-0.586
27	C	-0.122	-0.148	61	O	-0.622	-0.641
28	H	0.046	0.096	62	O	-0.584	-0.562
29	C	-0.041	-0.121	63	H	0.298	0.381
30	H	0.060	0.120	64	H	0.330	0.346
31	C	-0.075	-0.113	65	H	0.345	0.331
32	H	0.081	0.098	66	O	-0.658	-0.685
33	C	-0.073	-0.098	67	H	0.298	0.352
34	H	0.097	0.093	68	H	0.288	0.345

Table 6 — Relative deviation (RD) of frequency values of BLPAMA taken from experimental FTIR spectrum and MO6 DFT with 6-31++G(D,P) basis set (theoretical)

Bond types	IR Range (cm^{-1})	Experimental (cm^{-1})	Theoretical (cm^{-1})	RD=(V_{Theo} - V_{Exp}) * 100 / V_{Exp}
C=O	1730-1645	1712	1769	3.329
C-N	1350-1000	1194	1183	-0.083
N-H asymstret	3400 - 3000	3588	3309	-7.776
CH_2asym	3000 ± 50	2969	3089	4.042
CH_2 bending	1350-1250	1322	1464	10.741
COO^- symstret	1450 ± 50	1496	1630	8.957
NH_3^+ deformation	1550 ± 50	1570	1651	5.159
H-bonded OH stret	3100-2400	2831	2880	1.731
acid OH bend	1440-1400	1260	1437	14.048
acid C-O stret	1320-1210	1145	1099	-4.018

Table 7 — FTIR band assignment in BLPAMA

S. No.	Wave No.	Reduced mass	Force constant	Intensity	Vibration assignment
1	478	1.731	0.233	5.637	Ring wagging
2	524	4.325	0.699	37.701	γ CCH
3	628	5.587	1.300	4.919	β CCC, γ NCO, β CCN
4	750	2.070	0.686	222.543	γ C=O
5	884	1.128	0.519	59.277	Ring pluckering
6	893	2.733	1.285	17.708	γ CH
7	947	1.811	0.957	10.656	

(*Contd*.)

Table 7 — FTIR band assignment in BLPAMA (*Contd.*)

S. No.	Wave No.	Reduced mass	Force constant	Intensity	Vibration assignment
8	1017	1.740	1.061	4.118	*β* CNH, *β* NCO
9	1059	1.958	1.293	9.470	*β* CNH, *β* NCO
10	1099	1.541	1.098	19.122	*β* CCN
11	1105	1.651	1.188	16.499	Ring deformation
12	1189	1.248	1.039	26.645	*β* CH
13	1216	1.529	1.332	3.450	*β* CH
14	1283	2.092	2.028	16.185	*β* CN
15	1307	1.570	1.581	1.123	*t* CH2
16	1332	1.624	1.698	15.794	*β* CH
17	1367	4.444	4.890	7.568	*β* CCH
18	1389	1.577	1.791	16.053	*β* CH
19	1398	2.565	2.952	62.966	*ω* CH2
20	1464	1.556	1.964	211.669	*v* C-N
21	1472	1.332	1.699	114.793	*v* C-N
22	1608	1.037	1.579	78.442	*β* NH
23	1630	1.110	1.737	101.142	*β* NH
24	1650	2.987	4.791	36.001	*β* NH
25	1680	1.107	1.841	101.786	*v* C=O
26	3012	1.068	5.708	29.040	*v O-H*
27	3096	1.087	6.139	58.845	*v O-H*
28	3138	1.089	6.317	17.302	*v* CH
29	3149	1.089	6.362	14.949	*v* CH
30	3165	1.086	6.409	6.610	*v* CH
31	3186	1.093	6.537	34.150	*v* CH
32	3194	1.097	6.591	24.769	*v*s CH2
33	3200	1.099	6.628	16.571	*β* NH
34	3309	1.064	6.867	190.934	*v* CH
35	3533	1.068	7.858	539.838	*v* CH
36	3853	1.078	9.424	159.697	*v* NH

*v*s—sym stretching; *v*as—asym stretching; *β*—in plane bending; *γ*—out of plane bending; *ω*—wagging; *t*—twisting; *δ*—scissoring.

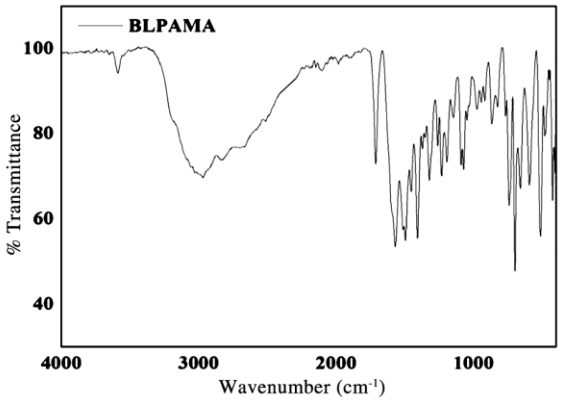

Fig. 4 — FTIR spectrum of BLPAMA

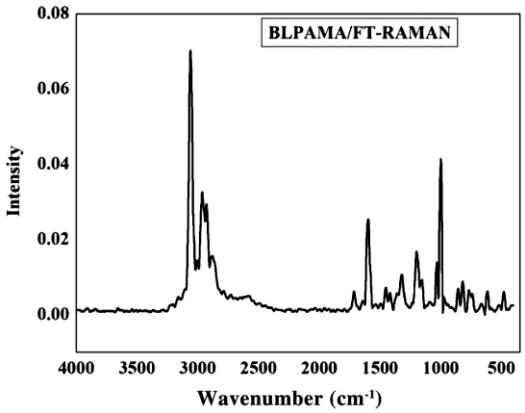

Fig. 5 — FT-Raman spectrum of BLPAMA

Rydberg non - Lewis electrons and the respective charge distribution resulting in the formation of neutral organic salt.

Natural Hybridisation Orbitals (NHO) show the deviations happening during the donor - acceptor interaction resulting in the bond bending and are given in the Table 10. The pi electrons in the bonding orbitals of C-O show higher angular deviation resulting in the formation of Vander Waals forces of attraction[6]. The antibonding orbitals of C-O show comparatively low angular deviation due to the intramolecular charge transfer. The C-C NBO close to hydrogen bonding orbitals show higher angular deviations compared to the C-C NBO at a distance.

As the angular deviation decreases the interaction between the bonding orbitals increases and give the formation of NHO (Ref. 7).

The second order Fock matrix is carried out to evaluate the donor–acceptor interactions in the NBO analysis. The interactions result in a loss of occupancy from the localized NBO of the idealized Lewis structure into an empty non-Lewis orbital. Table 11 indicates the energy changes involved in the donor-acceptor interactions happening in the four molecular units in the crystal. The hyper conjugative interaction of the C-C bonding donor orbitals, with the C-C anti bonding acceptor orbitals results in the higher stabilisation energy[8,9]. The donor-acceptor interaction of BD*(2) C27 - C29 donor anti bonding orbital with acceptor BD*(2) C26 - C35 show very high stabilisation energy of 294.65 KJ/mol. due to the π* enhanced hyper conjugative interaction. The donor LP (3) O 61 within unit 3 (second phenylalanine) to that of acceptor BD*(2) C43 - O 62 anti-bondingorbital, leads to second highest stabilization energy of 89.09 KJ/mol due to the hyper conjugative interaction of lone pair of electrons.

Table 8 — Comparison of FT-IR and FT-Raman in BLPAMA

S. No.	FT-IR	FT-Raman	Vibration assignment
1	478	482	Ring wagging
2	628	619	*β* CCC, *γ* NCO, *β* CCN
3	750	768	*γ* C=O
4	884	858	Rling pluckering
5	1017	1001	*β* CNH, *β* NCO
6	1189	1200	*β* CH
7	1307	1320	*t* CH2
8	1464	1451	*ν* C-N
9	1608	1603	*β* NH
10	1680	1714	*γ* C=O
11	3012	2963	*ν O-H*
12	3096	3059	*ν O-H*

*ν*s—sym stretching; *ν*as—asym stretching; *β*—in plane bending; *γ*—out of plane bending; *ω*—wagging; *t*—twisting; *δ*—scissoring

Frontier molecular orbital analysis

The energy gap between the Highest Occupied Molecular Orbital (HOMO) and the Lowest Unoccupied Molecular Orbital (LUMO) is found to be minimum which indicates the low chemical stability and high chemical reactivity of the compound BLPAMA[10-12]. The strong hydrogen bonding interactions lead to the low energy difference between HOMO - LUMO**.** The HOMO-LUMO plots of BLPAMA are shown in Fig. 6 and Fig. 7.

NMR spectral analysis

The ^{1}H NMR and ^{13}C NMR measurements are carried out for BLPAMA by dissolving it in the deuterated water and in the gaseous phase using

Table 9 — Natural population analysis (NPA)

Unit no	Mol. Formula	Total Lewis electrons %	Valence non- Lewis electrons %	Rydberg non-Lewis electrons %	Total unit %	Charge
1	$C_8H_8O_3$	97.6039	2.2032	0.1929	100	-0.03498
2	$C_9H_{11}NO_2$	97.4878	2.3111	0.2041	100	0.00614
3	$C_9H_{11}NO_2$	97.5642	2.2303	0.2055	100	0.01256
4	H_2O	99.4789	0.4447	0.0764	100	0.01628

Table 10 — NHO Directionality and "Bond Bending"(deviations from line of nuclear centers)
[Thresholds for printing: angular deviation > 1.0 degree]

hybrid *p*-character > 25.0% orbital occupancy > 0.10e

NBO	Line of centres Pi	Theta	Pi	Deviation	Theta	Pi	Deviation
BD(2)C1-O17	291.1	116.7	224.6	84.5	122.5	215.5	85.6
BD(2)C4-C5	355.3	26.1	297.8	90.2	26.4	298.7	90.4
BD(2)C7-C9	111.0	154.6	117.0	89.7	24.9	299.2	90.3
BD(2)C11-C13	230.2	24.8	299.9	90.4	154.8	118.3	89.7
BD(2)C20-O38	118.4	109.1	205.6	87.8	107.2	210.6	87.5
BD(2)C43-O62	2.6	130.8	299.7	81.9	137.0	280.5	83.0
BD(2)C49-C58	145.2	103.2	236.8	90.2	103.2	235.6	90.9
BD(2)C50-C52	163.0	77.0	56.4	89.9	102.8	235.8	90.4
BD(2)C54-C56	118.9	77.1	56.0	90.1	77.3	56.1	90.1
BD*(2)C1-O17	291.1	116.7	224.6	84.5	122.5	215.5	85.6
BD*(2)C4-C5	355.3	26.1	297.8	90.2	26.4	298.7	90.4
BD*(2)C7-C9	111.0	154.6	117.0	89.7	24.9	299.2	90.3
BD*(2)C20-O38	118.4	109.1	205.6	87.8	107.2	210.6	87.5
BD*(2)C43-O62	2.6	130.8	299.7	81.9	137.0	280.5	83.0
BD*(2)C49-C58	145.2	103.2	236.8	90.2	103.2	235.6	90.9

Table 11 — Second order perturbation theory analysis Fockmatrix in NBO basis

Threshold for printing: 0.50 kcal/mol

(Intermolecular threshold: 0.05 kcal/mol)

	Donor NBO(i)	Acceptor NBO(j)	E(2) (kcal/mol)	E(j)-E(i) (a.u.)	F(i,j) (a.u.)
within unit 1	BD (2) C 4 - C 5	BD*(2) C 7 - C 9	22.46	0.29	0.072
	BD (2) C 7 - C 9	BD*(2) C 11 - C 13	22.23	0.29	0.072
	CR (1) O 17	RY*(1) C 1	6.37	19.75	0.318
	LP (2) O 17	BD*(1) C 1 - C 2	19.46	0.67	0.104
	LP (2) O 17	BD*(1) C 1 - O 15	35.34	0.65	0.137
from unit 1 to unit 2	BD (1) C 1 - O 17	RY*(3) C 31	0.1	1.85	0.012
	BD (2) C 7 - C 9	BD*(1) C 33 - H 34	0.18	0.7	0.011
	BD*(2) C 1 - O 17	BD*(2) C 27 - C 29	0.46	0.02	0.005
from unit 1 to unit 3	BD (1) C 9 - H 10	RY*(1) H 57	0.2	1.17	0.014
	BD (1) C 9 - H 10	BD*(1) C 56 - H 57	0.37	0.97	0.017
from unit 1 to unit 4	BD (1) C 5 - H 6	BD*(1) O 66 - H 67	0.34	1.01	0.017
	LP (2) O 17	BD*(1) O 66 - H 68	2.63	0.8	0.042
from unit 2 to unit 1	BD (2) C 20 - O 38	BD*(1) C 5 - H 6	0.16	0.83	0.01
	LP (1) O 38	BD*(1) C 5 - H 6	0.21	1.16	0.014
	BD*(2) C 20 - O 38	BD*(2) C 4 - C 5	0.07	0.03	0.002
within unit 2	BD (1) C 20 - C 21	RY*(1) C 23	1.72	1.68	0.048
	BD (1) C 21 - H 22	BD*(2) C 20 - O 38	4.15	0.56	0.047
	BD (1) C 21 - H 22	BD*(1) N 37 - H 40	2.14	0.92	0.04
	BD (1) C 23 - C 26	BD*(1) C 21 - N 37	2.48	0.89	0.042
	BD*(2) C 27 - C 29	BD*(2) C 26 - C 35	294.65	0.01	0.084
from unit 2 to unit 3	LP (1) O 38	BD*(1) N 60 - H 64	2.29	1.07	0.044
from unit 2 to unit 4	LP (2) O 38	BD*(1) O 66 - H 67	2.45	0.76	0.039
from unit 3 to unit 1	BD (1) C 56 - H 57	BD*(1) C 9 - H 10	0.16	0.98	0.011
	BD (1) C 58 - H 59	RY*(1) H 8	0.08	1.2	0.009
from unit 3 to unit 2	LP (1) O 61	BD*(1) N 37 - H 40	16.78	1.01	0.117
	LP (2) O 61	BD*(1) N 37 - H 40	18.7	0.71	0.104
within unit 3	BD (2) C 49 - C 58	BD*(2) C 50 - C 52	20.07	0.31	0.07
	BD (2) C 49 - C 58	BD*(2) C 54 - C 56	21.47	0.3	0.072
	LP (3) O 61	BD*(2) C 43 - O 62	89.09	0.32	0.151
from unit 3 to unit 4	None above threshold				
from unit 4 to unit 1	BD (1) O 66 - H 68	BD*(1) O 18 - H 19	1.38	1.23	0.037
	LP (2) O 66	BD*(1) O 18 - H 19	21.56	0.87	0.122
from unit 4 to unit 2	BD (1) O 66 - H 67	BD*(1) C 20 - O 38	0.15	1.3	0.013
	LP (2) O 66	RY*(3) C 26	0.14	1.23	0.012
	LP (2) O 66	BD*(1) C 21 - H 22	0.18	0.78	0.011
	LP (2) O 66	BD*(1) C 21 - N 37	0.15	0.62	0.009
from unit 4 to unit 3	None above threshold				
within unit 4	LP (2) O 66	RY*(2) H 67	1.08	2.79	0.05
	LP (2) O 66	RY*(2) H 68	1.07	2.78	0.049

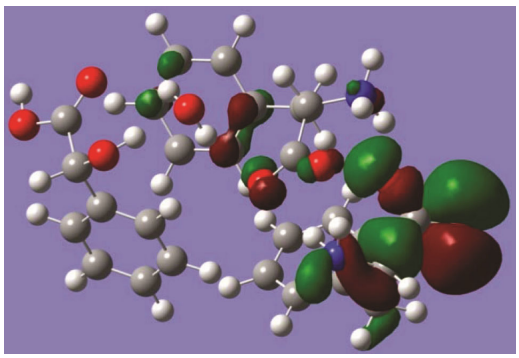

Fig. 6 — BLPAMA HOMO plot

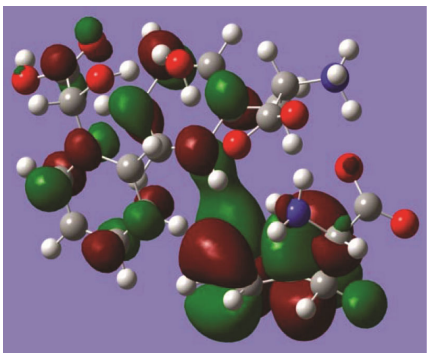

Fig. 7 — BLPAMA LUMO plot

Table 12 — ^{1}H NMR of BLPAMA (ppm)

BLPAMA	Experimental	Theoretical
Solvent	D_2O	-
Solvent peak	4.6-4.7	-
N-H Proton	2.90	2.24
CH_2 Proton	3.10	4.03
CH Proton	3.80	4.3
C-OH Proton	5.10	5.3
Aromatic proton	7-8	7-8
COOH Proton	-	9.6

Table 13 — ^{13}C NMR of phenyl alanine mandelates (PPM)

BLPAMA	Experimental	Theoretical
Solvent	D_2O	
Solvent peak	-	-
C - H Carbon	36.2	47.5
C-N Carbon	55.7	106
C - OH Carbon	73.4	143
Aromatic Carbon	120-140	120-140
Acid carbon	173.0	178
O=C-O anion	177.0	179

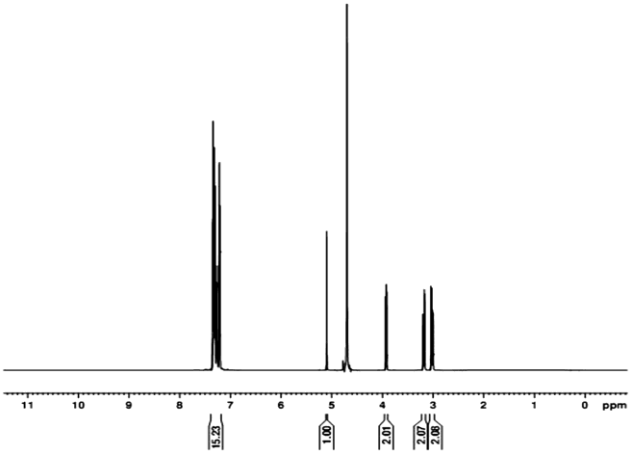

Fig. 8 — ^{1}H NMR of BLPAMA

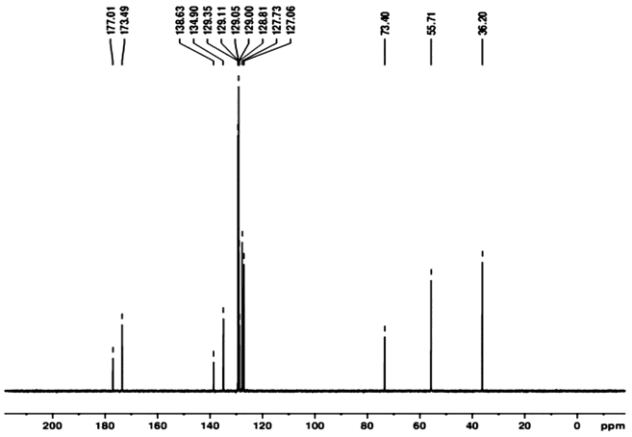

Fig. 9 —

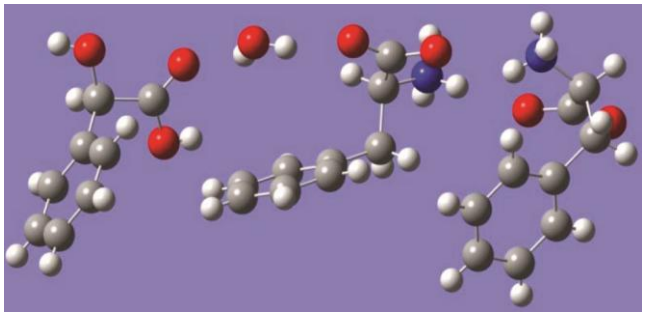

Fig. 10 — XRD structure of bis-L-phenylalanine mandelate (BLPAMA)

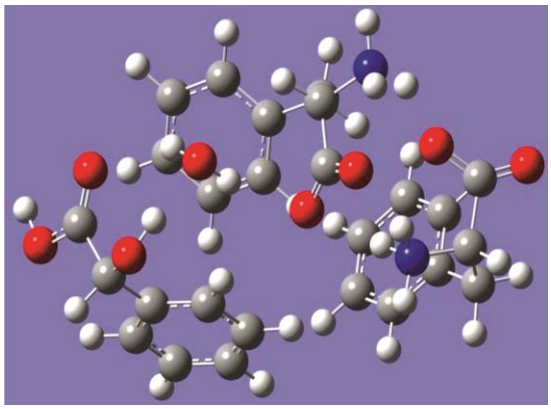

Fig. 11 — DFT structure of bis-L-phenylalanine mandelate (BLPAMA)

computational analysis. The comparative experimental and theoretical chemical shift values are given in Table 12 and Table 13. Both the measurements show small variations in the chemical shift; deshielded protons are observed in the upfield and shielded protons in the down field and are shown in Fig. 6 and Fig. 7 respectively. Multiplet is obtained for the eighteen aromatic carbons at 127-129 ppm and 15 aromatic protons at 7-7.5 ppm experimentally.

The variations in the experimental and theoretical values of chemical shifts are due to the disorderly arrangement of the units in the gaseous phase in the molecular crystal compared to the orderly arrangement of units in the solid phase measurement Fig. 8, Fig. 9, Fig. 10 and Fig. 11.

Absorption spectrum

The UV absorption spectrum of BLPAMA in Fig. 12, shows λ_{max} value at 212.9 nm and small absorption humps at 255-270 nm due to the different $\pi \rightarrow \pi^*$ transitions, and delocalisation of electrons in the aromatic ring structure[13].

The DFT - UV study of BLPAMA, Fig. 13 shows the higher excited state variation in plotting the oscillator strength *versus* wavelength and the λ_{max}

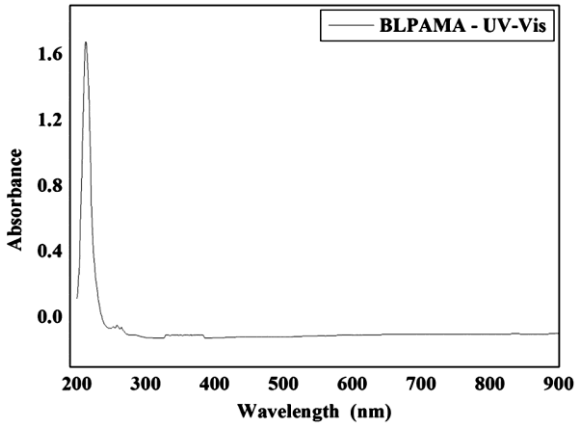

Fig. 12 — UV absorption spectrum of BLPAMA

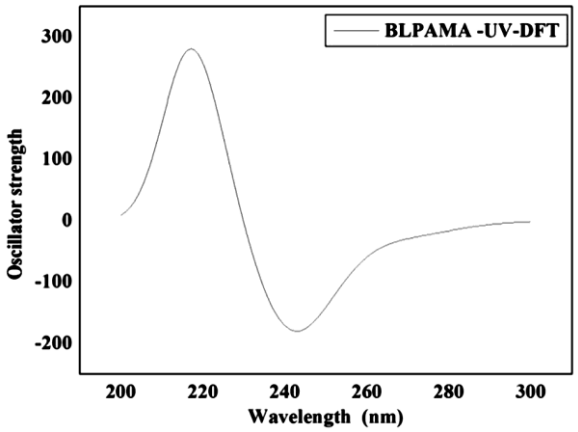

Fig. 13 — Plot of BLPAMA oscillator strength *versus* wavelength

seems to be 221 nm. The reason for this variation may be the disorderly alignment of individual units present in the BLPAMA in the gaseous phase measurement. There is no absorption in the visible region indicating the suitability of BLPAMA for optoelectronic application.

SHG property and NLO activity

The non-linear and non centerosymmetric structure, optoelectronic property, hyper conjugation and high thermal stability of BLPAMA indicates the possibility of SHG property and NLO activity in the novel organic salt. It is confirmed by subjecting the BLPAMA to Kurtz and Perry method and obtains about 56% NLO activity compared to standard NLO material KDP[14,15]. The reason for less NLO activity may be due to the evaporation of interstitial water molecules in the molecular crystal.

Conclusion

The four-component molecular crystal shows the suitability for optoelectronic applications. The theoretical study and experimental study comparison indicates the donor acceptor mechanism leading to charge transfer in the case of gaseous state and solid state of the title compound, provides the suitability of the compound for biological activities.

Acknowledgments

I acknowledge the support rendered by IIT-M department of chemistry for the computational analysis and the constant encouragement of the management of Sri Sairam Engineering College.

References

1 Usha S & Christopher C K, *Chem Sci Trans*, 5 (1) (2016) 179.
2 Senthil Kumar J & Arivazhagan M, *Indian J Pure Appl Physics*, 49 (2011) 673.
3 Kerruetal N, *Scientific Reports*, 9 (2019) 19280.
4 Nagy I P, *IJMS*, 15 (2014) 19562.
5 Muthu S, Prasath M, Arun Balaji R & Uma Maheswari J, *Int J Engineering*, Tome X (2012) 399.
6 Usha S & Christopher C K, *Materials Today*: *Proceedings*, 16 (2019) 1137.
7 Gangadharan R P & Krishnan S S, *Acta Physica Polonica A*,125 (1) (2014) 18.
8 Chandra Sekhar M, Venkatesulu A, Madhu Mohan T & Gowrisankar M, *Oriental J Chem*, 31 (2) (2015) 897.
9 Tighadouini S, Benabbes R, Tillard M, Eddike D, Haboubi K, Karrouchi K & Radi S, *Chemistry Central J*, 12 (2018) 122.
10 Djurovich P I, Mayo E I, Forrest S R & Thompson M E, *Org Electronics*, 10 (2009) 515.
11 Khan S A, Obaid A Y, Al-Harb L M, Arshad M N, Asiri A M & Hursthouse M B, *Int J Electrochem*, 10 (2015) 2306.
12 El Alamy A, El Ghayoury A, Amine A & Bouachrine M, *Journal of Taibah University for Science*, 11 (2017) 930.
13 Zara Z, Iqbal J, Ayub K, Irfan M, Mahmood A, Khera R A & Eliasson B, *J Mol Str*, 1149 (2017) 282.
14 Alver O, Senyel C P M, *Bull Chem Soc Ethiopia*, 23 (3) (2009) 437.
15 Mahadevan M & Ramachandran K, *IJIRSET*, 3 (1) (2014) 8785.